



City Research Online

City, University of London Institutional Repository

Citation: Hantschke, M. & Triantis, I. F. (2022). Optimisation of an Electrical Impedance Sensor for Use in Microfluidic Chip Electrophoresis. *IEEE Sensors Journal*, 22(1), pp. 16-24. doi: 10.1109/jsen.2021.3127320

This is the accepted version of the paper.

This version of the publication may differ from the final published version.

Permanent repository link: <https://openaccess.city.ac.uk/id/eprint/34490/>

Link to published version: <https://doi.org/10.1109/jsen.2021.3127320>

Copyright: City Research Online aims to make research outputs of City, University of London available to a wider audience. Copyright and Moral Rights remain with the author(s) and/or copyright holders. URLs from City Research Online may be freely distributed and linked to.

Reuse: Copies of full items can be used for personal research or study, educational, or not-for-profit purposes without prior permission or charge. Provided that the authors, title and full bibliographic details are credited, a hyperlink and/or URL is given for the original metadata page and the content is not changed in any way.

City Research Online:

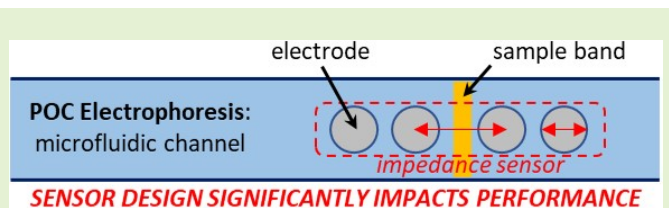
<http://openaccess.city.ac.uk/>

publications@city.ac.uk

Optimisation of an Electrical Impedance Sensor for use in Microfluidic Chip Electrophoresis

Martin Hantschke, *Member, IEEE*, Iasonas F. Triantis, *Senior Member, IEEE*

Abstract—Label-free measurements using impedance sensing could enable microfluidic chip electrophoresis (ME) to be used in point-of-care (POC) diagnostics. However, impedance sensing methods reported in this field need considerable optimisation. **GOAL:** Develop a novel design process for optimising tetrapolar electrical impedance measurement (TEIM) sensor performance in ME applications through a systematic investigation a) of the impact of a TEIM sensors design parameters on its performance in ME and b) of the relationship between the above parameters with those of the microfluidic channel and the sample to be sensed. **METHODS:** 3D FEM sensitivity simulations, verified experimentally, were carried out to study the impact of sensor and channel parameters on the measured impedance and their interrelationship. Subsequently, the impact of sensor parameters on sensing a sample band's conductivity and size was investigated. **RESULTS:** The impact of channel dimensions on transfer impedance measurements is significant. The non-linearity reported for transfer impedance measurement of volume conductors can be manipulated by appropriate sensor parameter design. The sensor performance can be optimised by designing electrode length and measurement electrode distance in relation to the channel height and sample band length, respectively. The sensor performance is not affected by the injection electrode distance. **CONCLUSION:** There is a relationship between sensor, channel and band parameters and this warrants establishing a systematic design process of TEIM sensors in ME. **SIGNIFICANCE:** This paper presents a novel approach to optimising the design of TEIM sensors in ME potentially providing significant performance improvements and thus allowing for label-free POC electrophoresis diagnostics.



Index Terms—Tetrapolar, Impedance, Sensitivity, Microfluidics, Electrophoresis, Cell constant, Conductivity Detection.

I. INTRODUCTION

Microfluidic chip electrophoresis (ME) is a very important and still emerging analytical method for clinical diagnostics used in a wide range of applications such as genomics, forensics and biomarker analysis [1]. The simple functional principle, cost effective process, quick analysis and minimal sample volume makes ME a very viable alternative to more cumbersome yet very established methods such as high performance liquid chromatography (HPLC) and gas chromatography (GC) [2]. Additionally the front-end's reduced dimensions can be combined with appropriate sensing methods to improve portability and allowing for its application in point-of-care (POC) devices [3]. The most commonly used detection method in ME, laser-induced fluorescence (LIF), requires a fluorescent analyte and with autofluorescence being rare, fluorescent labelling has to be applied to the biological sample [4]. However the elaborate and potentially hazardous nature of pre- or post-labelling processes [2] requires a laboratory setting with trained personnel thus limiting the use of LIF for POC. Conductivity detection (CD) - including the emerging capacitively-coupled contactless conductivity detectors (C^4D) - has been recognised as a potential alternative sensing method for POC implementations of ME due to its label-free, cost

effective and compact design, whose operation does not require a specialist operator or a bespoke laboratory [1]. As it is concerned with the sample's electrical properties and although the sample is usually considered purely resistive, CD is a sub-category of electrical impedance or sensing, also labelled transfer impedance in [5]. It has been used in electrophoresis for more than three decades, however its detection performance in terms of measurement sensitivity or perceptivity - is inferior to LIF by up to six orders of magnitude [6] effectively hindering the wider development of POC ME devices.

Bipolar impedance measurements featuring in the majority of CD in ME literature - use a pair of electrodes for injecting current and measuring voltage and their performance is significantly degraded by the electrode contact impedance. That can be minimised through the use of tetrapolar (four electrode) electrical impedance measurement - henceforth termed TEIM. The method features separate pairs of electrodes used respectively for applying the ac signal and for measuring the response [7]. Tetrapolar sensors have been used - to the authors' knowledge - only twice in ME [8], [9] claiming improved perceptivity and limit of detection over bipolar ones, although still without reaching the performance of LIF.

It is therefore very desirable to discover ways by which TEIM sensors can be optimised so as to be used for label-free POC applications with satisfactory performance. Studies on applications outside the field of electrophoresis [10]

M. Hantschke and I. F. Triantis are with the Research Centre for Biomedical Engineering (RCBE), City, University of London, Northampton Square, London EC1V 0HB, United Kingdom; emails: martin.hantschke.1@city.ac.uk, i.triantis@city.ac.uk

[11] indicate that impedimetric sensors' performance can be improved by adjusting the electrode geometric parameters. Still, besides a few studies [12] [13] [14], little attention has been paid to the electrode design in bipolar - and even less in tetrapolar - impedance sensing methods used in ME.

Although not systematically approached, the hypothesis that the "sensor" parameters have impact on the measurements in ME has been strengthened through the findings of several studies [13], [15], [16], [12], [17] albeit for bipolar sensors. These studies were mostly empirical with some analytical approaches made on the assumption that impedance sensors properties can be adequately described by the cell constant theory. The cell constant, the relationship of measured resistance and the resistivity of the electrolyte, is generally formulated for the geometric dimensions of a parallel bipolar topology. This however is not an adequate representation of interfaces used in microfluidics, where the electrodes are e.g. co-planar [18] or whenever tetrapolar electrodes are used. Studies assessing adaptations of the cell constant for coplanar electrodes [15] [12] observed poor agreement between calculations and experimental data.

In light of the above, with the electrode geometry being established as very influential to the measurement and with TEIM being preferable for eliminating the electrode contact impedance, a method needs to be developed for systematically designing optimised impedimetric sensors for ME applications.

An established method of investigating performance of bipolar and tetrapolar transfer impedance measurements in volume conductors is the lead field theory [19]. Using finite element method (FEM) to calculate the lead field product, Brown et al. [20] was able to show that, depending on the position relative to the electrodes, different regions volume contribute differently to the measured transfer impedance. This different contribution of volume elements within a larger volume is termed sensitivity distribution, or just "sensitivity"¹. Using sensitivity distribution in simulations it has been demonstrated [5] that, even in homogeneous media, the topology of the TEIM electrodes and especially the relative positioning of the injecting versus the measuring electrode pairs influences the measured impedance. This indicates that sensitivity distribution simulations can be used as a TEIM sensor design tool, effectively for optimising the electrode topology for use in ME.

This paper aims to demonstrate that impedance sensors for ME should be appropriately designed in relation to both the channel and the analyte. It investigates the relationship between the sensors parameters, namely electrode size and inter-electrode distances, with the parameters of the microfluidic channel and with the characteristics of the analyte and more specifically the sample bands. These parameters are found to have a significant impact in the sensor performance. Subsequently, for the first time in ME impedimetric (or CD) sensor design, a systematic design approach is proposed, based on sensitivity distribution simulations rather than on sensi-

tivity distribution simulations rather than through empirical approximations. Developing such design methods will pave the way for achieving label-free POC ME analytical tools, thus potentially changing the way in which biological samples are currently analysed and the time it takes for results to be generated.

As this paper is focused on the design of the sensor and its relationship to both the channel and the analyte, it is essentially a three-component study (with the three components being the sensor parameters, the channel parameters and the analyte parameters). It will therefore be carried out in two stages, with the first one studying the sensor-channel relationship with the analyte fixed and the second one fixing the channel and looking into the sensor response for analyte parameter variations. In the next sections we first investigate the effect of the channel dimensions on transfer impedance magnitude including experimental verification of the FEM results. Then the effect of electrode topology dimensions, specifically electrode length and electrode distance, on the transfer impedance magnitude is examined. We then investigate how these topology dimensions affect the measurement performance of electrolyte concentration in terms of transfer impedance and sample concentration changes to improve the perceptivity.

II. MATERIALS AND METHODS

A. Fabrication of microfluidic chips

Eleven microfluidic chips, all with outer dimensions of 75 mm x 25 mm x 6 mm and a 60 mm long separation channel, were manufactured in-house similarly to [22]. All of them featured an embedded tetrapolar impedance sensor. Each chip was designed with a different separation channel height and/or width, as detailed later. Figure 1a shows a representative microfluidic chip including the separation channel (henceforth mentioned as 'channel') with the tetrapolar sensor and a shorter injection channel in a common cross channel design [3]. As shown in the diagram and the micro-photograph in figure 1b the tetrapolar sensor comprised four Pt wires with their endings forming electrodes flush with the upper channel surface. It was positioned near the end of the channel, at about 1 mm distance from the waste reservoir, as typically done with electrophoresis sensors [23] to maximise the effective separation channel length. The channel section bearing the electrodes, shown in figures 1b and 1c is henceforth called the 'sensing region'².

Each microfluidic chip was constructed from two 3 mm thick PMMA (polymethylmethacrylate) slides. One slide featured the electrodes and access holes to the channel, which were drilled using CNC milling. The other slide featured the channel, with 11 different versions fabricated using moulds on glass slides, which were made by photolithography and wet etching. The channel structure was imprinted by hot embossing and sealed with the top plate using isopropyl alcohol (IPA) assisted bonding. Two sets of moulds were fabricated, one set

¹Please note this does not relate to the term "sensitivity" used in sensors and instrumentation which, as suggested in [21], is named **perceptivity** in this work to avoid confusion.

²In subsequent figures the electrodes are displayed as being at the bottom of the channel (z-axis mirror view) and the centre of the tetrapole is used as the x-axis origin.

with fixed channel width of $80 \mu\text{m}$ and 5 different heights ($h_{ch} = \{30, 40, 50, 60, 80\} \mu\text{m}$) and the other designed with fixed channel height of $50 \mu\text{m}$ and 6 six different widths ($w_{ch} = \{50, 70, 100, 120, 150, 200\} \mu\text{m}$). They were measured post-experimentally through cross-sectional cutting of the PMMA channels and found to exhibit an average error of $\pm 5 \mu\text{m}$.

In this study electrode tetrapoles (sets of four electrodes in line with each other) were fabricated and simulated. They were placed in direct contact with the separation channel similar to in-contact electrode pairs reported in bipolar impedance sensors [12] [24]. The electrodes were made of platinum wire with diameter $d_{el} = 127 \mu\text{m}$ inserted through holes drilled in the PMMA slide. These were drilled in line, along the channel axis, spaced at $200 \mu\text{m}$ centre to centre, resulting in $73 \mu\text{m}$ electrode edge to edge distance. The wires were immobilised inside the holes of the top plate and sealed with superglue, then sanded and polished to be flush with the inner channel surface. The electrode positions and the channel dimensions were visually confirmed with photo mask rulers under the microscope. An example of the wire electrodes is shown in the microphotograph of Fig. 1b.

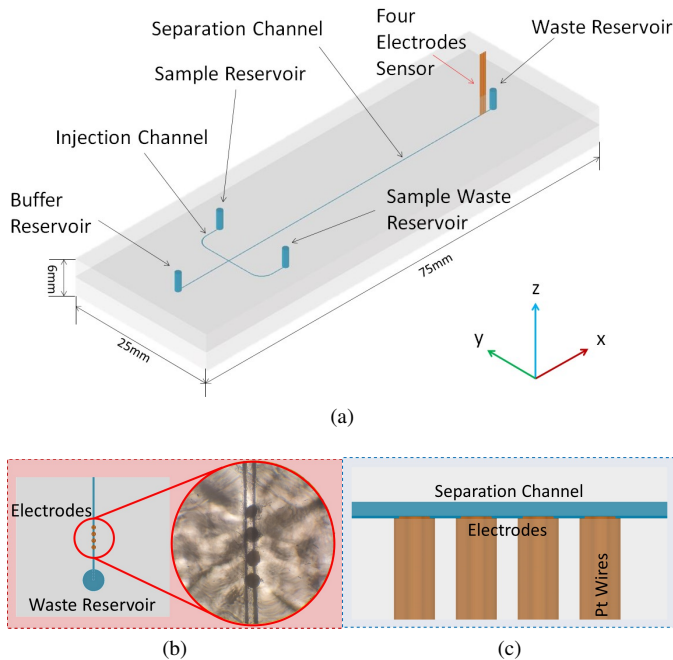


Fig. 1: Schematic of the microfluidic chip with the Pt wire electrodes sensor. (a) Overall view; (b) Top view of the sensor with a microphotograph of the highlighted region showing the 4 electrodes; (c) Side view of the highlighted region (the "sensing region").

B. Experiment

Experiments were carried out using 0.9% w/v NaCl solution as background electrolyte. The conductivity of the NaCl solution was $\sigma = 1.74 \text{ S/m}$, evaluated using a conductivity meter (Jenway 3540). The channel was filled with NaCl via pressure injection employing plastic syringes prior to the experiments. The syringe was disconnected during the experiments. Before

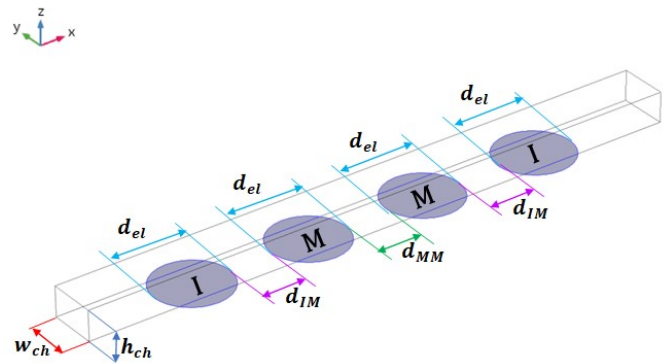


Fig. 2: Diagram of a 1 mm long sensing region model, with $h_{ch} = 50 \mu\text{m}$ and $w_{ch} = 80 \mu\text{m}$. Injection (I) and measurement (M) electrodes feature inter-electrode distances $d_{MM} = d_{IM} = 73 \mu\text{m}$ and diameter $d_{el} = 127 \mu\text{m}$ (matching the fabricated sensor). The surrounding PMMA material is omitted.

each measurement the channel was flushed and cleaned with ca 1 ml de-ionised water and emptied after the experiments. The platinum electrode wires were connected through custom shielded connectors with micro clamps to a Precision LCR Meter (Keysight E4980). The LCR meter was connected to a PC via the ethernet port and MATLAB was used for the instrument control, as well as for data acquisition and data processing. The 11 home made microfluidic chips, each of different cross-sectional channel dimensions and featuring a TEIM sensor, were connected in turn to the analyser. For each TEIM sensor current was injected through the two outer electrodes - henceforth called the injection (I) electrodes - and voltage was measured across the two inner ones - the measuring (M) electrodes. In accordance to the literature [8], the injected signal frequency was set at 10 kHz.

C. FEM simulations

FEM simulations were carried out using COMSOL Multiphysics V5.3 following the procedure in [25]. The 3D microfluidic chip model (Fig. 2) was made identical to the sensing region of the fabricated physical chip (Fig. 1a). It comprised a $1000 \mu\text{m} \times 1000 \mu\text{m} \times 1000 \mu\text{m}$ cube of PMMA ($\sigma = 10^{-19} \text{ S/m}$, $\epsilon_r = 2.6$) surrounding a NaCl ($\sigma = 1.74 \text{ S/m}$, $\epsilon_r = 80.1$) filled $1000 \mu\text{m}$ long microfluidic channel embedded in the centre of the slide. The reason for modelling and simulating only the sensing region (Fig. 1c and Fig. 2) was so as to minimise computational loading. Ranges of $h_{ch} = \{10 \text{ to } 200\} \mu\text{m}$ and $w_{ch} = \{10 \text{ to } 200\} \mu\text{m}$ were simulated with $10 \mu\text{m}$ increments, so as to include channel dimensions used in the experiments and also reported in literature for bipolar and tetrapolar conductivity detection in electrophoresis [8] [12]. The electrodes were designed as zero thickness platinum electrodes ($\sigma = 8.9 \times 10^6 \text{ S/m}$, $\epsilon_r = 1$) on the channel surface. All electrodes simulated in this paper were round except for the ones used in section II c where a rectangular shape allowed for the electrode length to be examined independently of its width. In line with standard practice in modelling TEIM sensors [10], electrode contact impedance has been omitted in

our model, given its minimisation by the tetrapolar method [7]. The model was meshed to 119,079 elements with an average element quality of 0.68. The simulations were conducted with the same frequency as the experiments (10 kHz). The sensitivity distribution S and the transfer impedance Z_{Tr} sensed by each different electrode tetrapole (TEIM sensor), are calculated from current density values generated in the AC-DC COMSOL module. The contribution of different regions within the volume conductor to the measured transfer impedance Z_{Tr} is provided, according to the lead field theory, by the volume integral in eq. 1:

$$Z_{Tr} = \int_V \rho S dV \quad (1)$$

The sensitivity S is defined as [7]:

$$S = \frac{\bar{J}_1 \cdot \bar{J}_2}{I^2} \quad (2)$$

where J_1 is the current density vector in the electrolyte when an external current I is injected through the current injecting electrodes and picked up by the voltage measuring electrodes and J_2 the reciprocal current density vector occurring when a current is injected through the voltage measuring electrodes and picked up by the current injecting electrodes.

III. EXPERIMENT AND SIMULATION RESULTS AND DISCUSSION

The experiments were carried out to investigate the influence of the channel cross-sectional dimensions on the transfer impedance. The first set of 5 microfluidic chips, constructed with different channel heights as detailed in Section II.A., was used. The distance between neighbouring pairs of the TEIM sensor electrodes was $d_{MM} = d_{MI} = 73 \mu\text{m}$, for all five chips. The channels were filled with electrolyte solution, as described earlier.

The resulting transfer impedance values for the range of simulated channel heights (h_{ch}) detailed in Section II.C. is presented along with the aforementioned experimental results in Fig. 3a. Both data trends indicate that the transfer impedance values obtained increase with decreasing channel height. The baseline of the experimental transfer impedance values is in general slightly higher than the simulated ones, possibly due to tolerances in the concentration of the electrolyte solution as well as in the in-house manufacturing process relative to the corresponding modelled parameters.

A similar set of experiments was carried out with the second set of 6 microfluidic chips of different channel widths described in Section II. A. The resulting transfer impedance values for the range of simulated channel widths (w_{ch}) detailed in Section II.C. is presented along with the aforementioned experimental results in Fig. 3b. They exhibit the same general characteristics as those obtained with h_{ch} variations, albeit with higher magnitudes due to the overall larger cross sectional area of the channels used for this set. The current density J is expected to be inversely proportional to the channel cross sectional area $A = w_{ch} \times h_{ch}$. Hence, Z_{Tr} should be inversely proportional to variations of either h_{ch} or w_{ch} . Based on this theoretical relationship the data in figures 3a and 3b were fitted in Matlab with a a/x type fit. It is seen

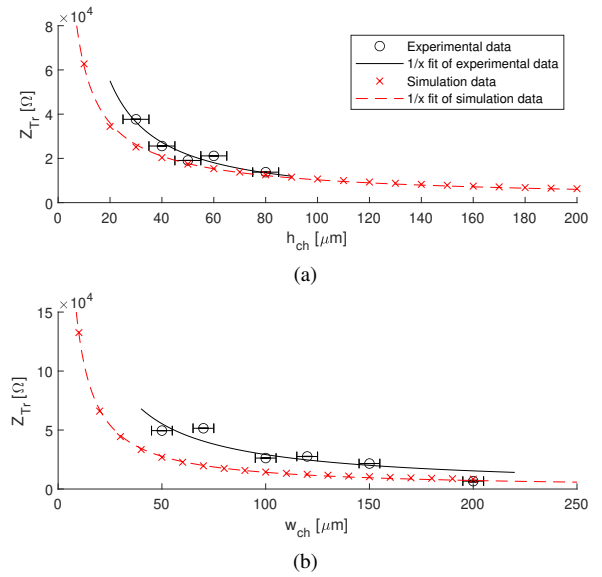


Fig. 3: Simulated and measured transfer impedance values as a function of (a) channel height, for channel width $w_{ch} = 80 \mu\text{m}$ and (b) channel width, for channel height $h_{ch} = 50 \mu\text{m}$. Other dimensions as in Fig. 2

that the fits are generally satisfactory, demonstrating that both the experimental and the simulation data follow the same type of trend. Since A is the product of height and width, we will henceforth further examine only h_{ch} .

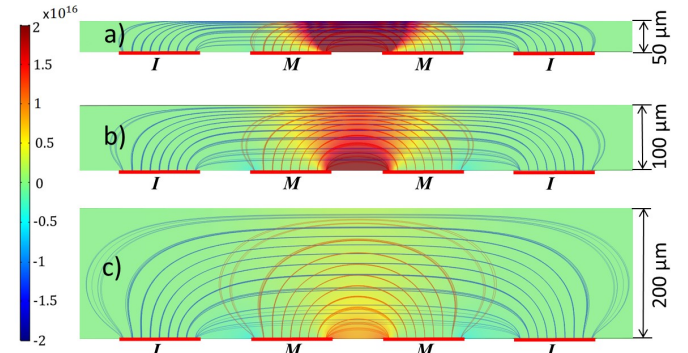


Fig. 4: Side view of the sensing region with x from -400 to $400 \mu\text{m}$, $d_{MM} = 73 \mu\text{m}$ and h_{ch} of: a) $50 \mu\text{m}$, b) $100 \mu\text{m}$, c) $200 \mu\text{m}$. Simulated electric field lines of J_1 (red) and J_2 (blue) overlaid on a sensitivity distribution rainbow colour map (units $1/m^4$).

The impact of channel height variation on the current density field and on the sensitivity distribution in the sensing region is illustrated in Fig. 4. The figures are generated from the same 3D simulations as the data presented in Fig. 3a and shown in the xz plane (see Fig. 1c). It is seen that the current density decreases as the channel height increases from subplot a) to c). Additionally the magnitude and distribution of the sensitivity is changing due to the effect of the channel dimensions on the current density vectors. The polarities of the current density vectors are based on the polarity defined

for the injection and measurement electrode pairs hence for the simulated configuration neighbouring I and M electrodes are assumed to have the same polarity. Increasing channel height affects the angle between the current density vectors J_1 and J_2 resulting in fewer vectors at 0° in the centre of the tetrapole and more at 180° between each of the neighbouring I and M electrodes, hence increasing the vector product. This causes the positive sensitivity magnitude to decrease and the negative sensitivity to increase in the respective 'red' and 'blue' coloured regions. The significantly reduced negative sensitivity for the channel dimensions used in ME is a notable conclusion as impedimetric measurements in electrophoresis, as reported in our previous work [26].

IV. FURTHER SIMULATION RESULTS AND DISCUSSION

The following simulations explore the effects of the TEIM sensor parameters (i.e. electrode dimensions and inter-electrode distances) on its performance and the relation of these parameters to the channel's width and height. In all cases the origin of the x-axis is fixed at the centre of the sensor.

A. Influence of electrode length on transfer impedance

In general it is desirable for electrodes placed in an electrophoresis channel to be as small as possible, given the averaging effect that a conductor will have on the separation field occurring over its surface. On the other hand too small electrodes will potentially degrade transfer impedance measurement due to thermal noise associated with smaller electrodes [27]. Hence it is essential to investigate how short the electrodes can be made without adverse effects and whether their minimum length is related on the height of the channel or the distance between the electrodes. The simulations in this section were carried out using rectangular electrodes with a width $w_{el} = 80 \mu\text{m}$, as wide as the channel. Initial evaluation showed that the sensitivity distribution is influenced by the sensor electrode lengths as shown in Fig. 5. The simulation results show that the conductor (electrolyte solution) transfer impedance originally increases as a function of electrode length and then reaches a maximum transfer impedance value plateau, as illustrated in Fig. 6a. We call *optimal length* L_X the electrode length at which the transfer impedance reaches 95% of the plateau value. Figs. 6a and 6b respectively show that L_X increases with channel height but is independent of the distance d_{MM} between the measurement electrodes. Fig. 7 shows the dependence of L_X on the channel height and indicates more clearly its independence on d_{MM} . It is seen that for channel heights between 10 and $190 \mu\text{m}$ the minimal electrode length exhibits a nearly linear relationship with h_{ch} with a slope of approximately 2. This leads us to introduce as a design rule for TEIM sensors in ME that the optimal electrode length for full width electrodes should be $2 \times h_{ch}$.

B. Influence of inter-electrode distance on transfer impedance

The impact of the measurement electrodes distance d_{MM} on the sensitivity distribution and on the transfer impedance was

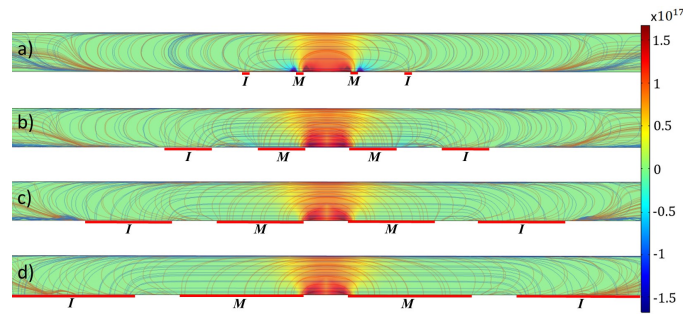


Fig. 5: Simulated volume sensitivity distribution in xz-plane view for the channel x region from -400 to $400 \mu\text{m}$, in rainbow colour and in units of $1/m^4$. The measurement electrode lengths are: a) $l_{el} = 10 \mu\text{m}$ b) $l_{el} = 60 \mu\text{m}$ c) $l_{el} = 110 \mu\text{m}$ d) $l_{el} = 160 \mu\text{m}$; other dimensions as in Fig. 2

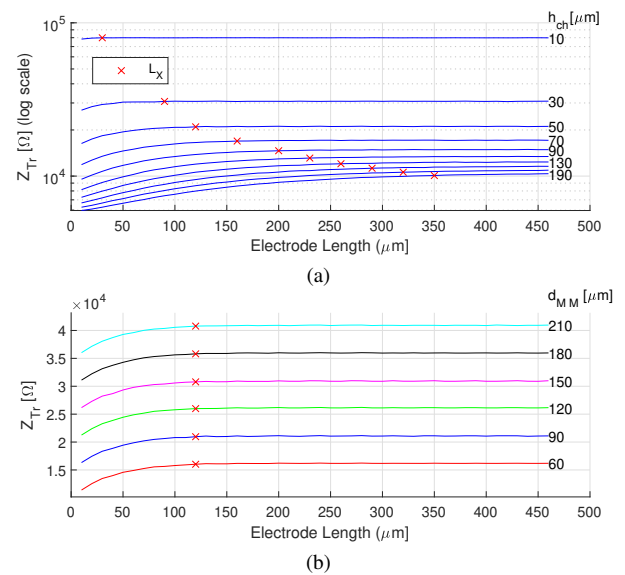


Fig. 6: a) Transfer impedance as a function of measurement electrode length for microfluidic channels with heights h_{ch} between 10 and $190 \mu\text{m}$, at constant measurement electrode (edge to edge) distance of $180 \mu\text{m}$; red x indicates L_X for each channel. b) Transfer impedance as a function of measurement electrode length for measurement electrode (edge to edge) distances d_{MM} between 60 and $210 \mu\text{m}$, at constant channel height $h_{ch} = 50 \mu\text{m}$

investigated by simulating measurement electrodes distances in $200 \mu\text{m}$ intervals starting from $73 \mu\text{m}$ (to match the aforementioned experimental setup) to $1673 \mu\text{m}$ and constant injection electrode distance of $d_{II} = 2073 \mu\text{m}$. Additionally these simulations were conducted for three different channel heights ($h_{ch} = \{50, 100, 150\} \mu\text{m}$) to examine d_{II} and d_{MM} variations in relation to h_{ch} . For each height the optimum L_X values were used.

The impact of the injection electrodes' distance d_{II} on the sensitivity distribution and on the transfer impedance was investigated by simulating d_{II} values between $473 \mu\text{m}$ and $2473 \mu\text{m}$ in $200 \mu\text{m}$ intervals, with $d_{MM} = 73 \mu\text{m}$. The results in Fig. 8a indicate that increasing d_{II} - using optimal

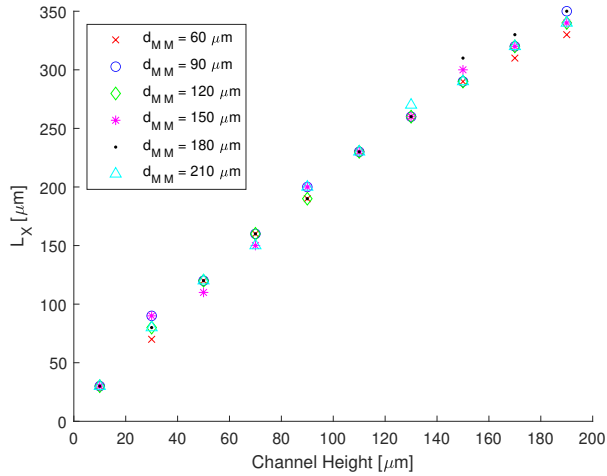


Fig. 7: Optimal electrode length L_X as function of channel height for different measurement electrode distances d_{MM}

electrode length - does not significantly affect the resulting transfer impedance as it does not change the current density contributing to the sensitivity distribution. The figure indicates that baseline impedance is inversely proportional to height variation, as also shown in figure 3a.

It can be observed in Fig. 8b that the transfer impedance increases linearly when increasing d_{MM} . When using electrodes with optimal electrode length L_X , the current density vectors are not changing with d_{MM} variations and thus the microfluidic channel may be treated as a thin linear conductor [7]. However, as indicated in figure 9, increasing d_{MM} does increase the regions of positive sensitivity between the measurement electrodes and thus the measured electrolyte volume resulting in increased transfer impedance. Direct proportionality of electrode distance and transfer impedance was reported in ME [13], albeit not clearly shown due to limited data points used.

C. Influence of electrolyte solution conductivity on transfer impedance

The results so far demonstrate how the value of transfer impedance measured by the TEIM sensor will vary in relation to parameters of either the channel or the sensor itself. However, as the conductivity of the solution inside the channel has thus far been constant, there is no indication as to whether these transfer impedance variations are simply baseline shifts or whether they relate to improvements in the sensor perceptivity. The latter would translate to higher transfer impedance difference once an analyte (e.g. a sample band) would pass over the sensor. In the subsequent simulations we examine how variations in the solution conductivity, either global or localised (sample band) - result to transfer impedance variations and how the latter changes with d_{MM} .

The simulations carried out show that the amount of decrease of transfer impedance for increasing electrolyte conductivity values depends on d_{MM} , as shown in Fig. 10a. Subtracting the individual baseline impedance values for this

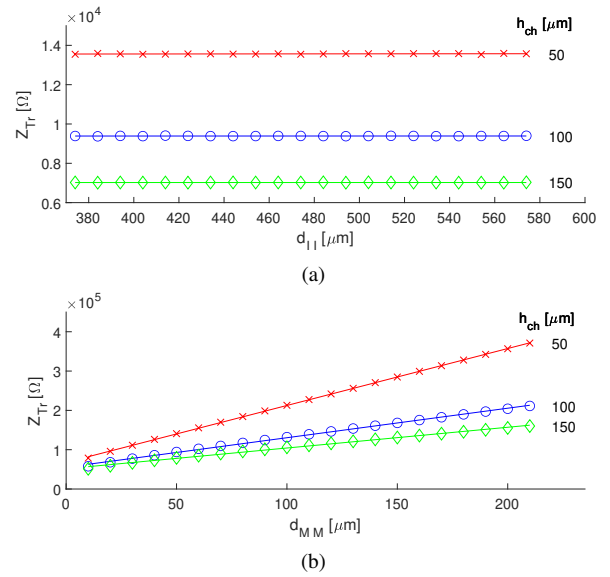


Fig. 8: a) Transfer impedance as a function of injection electrode distance (d_{II}) for different channel heights; constant measurement electrode distance of $d_{MM} = 73 \mu\text{m}$ b) Transfer impedance as a function of measurement electrode distance d_{MM} for different channel heights; constant injection electrode distance of $d_{II} = 2073 \mu\text{m}$; solid lines are linear fits of the data-points; other dimensions as in Fig. 2

data-set reveals that larger measurement electrodes distances are more perceptive to changes of the electrolyte conductivity (Fig. 10b). Hence, increasing d_{MM} can be advantageous as it improves the perceptivity and resolution, similar to the observations for bipolar configurations in [12].

The above observations imply that the perceptivity to changes of the electrolyte conductivity could be increased by simply increasing d_{MM} . On the other hand, increasing d_{MM} will reduce the spatial resolution when detecting sample bands in electrophoresis [13] [28]. Furthermore, for low conductivity electrolytes an excessive increase of the measurement electrodes distance would result to high baseline transfer impedance values (up to $\text{M}\Omega$ order), requiring high input dynamic range for the front electronics and thus making it difficult to detect the relatively small transfer impedance variations due to a band passing over the sensor [12]. Therefore it is of interest to find the optimum d_{MM} for a specific band length.

D. Influence of sample band conductivity on transfer impedance

In order to investigate how sensitivity distribution affects the spatial resolution in electrophoretic separations, a static sample band was simulated by generating a region of increased conductivity at the centre of the sensing region (see Fig. 9). The sample band width and height were equal to those of the channel and the band length l_b was $80 \mu\text{m}$. The sample band conductivity σ_b was varied by up to 10% relative to the electrolyte conductivity of $\sigma = 1.74 \text{ S/m}$. The results presented in Fig. 11a show that, in agreement with Fig. 10a, the transfer

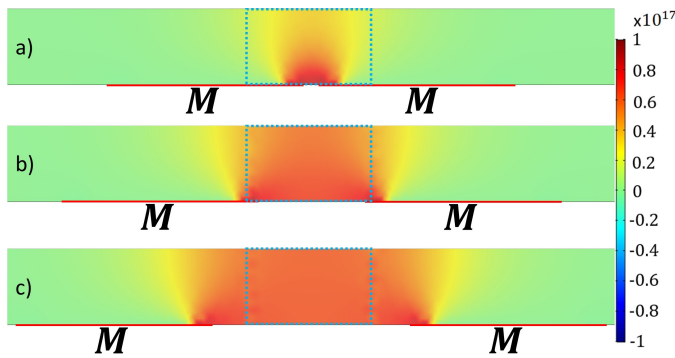


Fig. 9: Simulated volume sensitivity distribution, in rainbow colour and in units of $1/m^4$, for measurement electrode distance variation a) $d_{MM} = 10 \mu\text{m}$ b) $d_{MM} = 60 \mu\text{m}$ c) $d_{MM} = 120 \mu\text{m}$; z-x plane view of sensitivity distribution for the channel region with x from $-300 \mu\text{m}$ to $300 \mu\text{m}$; other dimensions as displayed in Fig. 2, sample band indicated by blue dashed rectangle

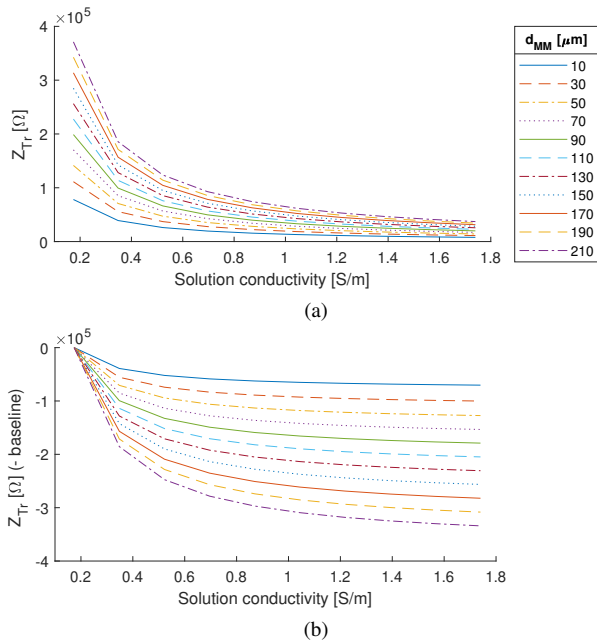


Fig. 10: Transfer impedance as a function of electrolyte conductivity for different values of the measurement electrodes distance d_{MM} (a) raw data (b) with individual baseline subtraction

impedance magnitude increases significantly with increased d_{MM} but is not significantly affected by sample conductivity variations. However, after subtracting the baseline of each trace (corresponding to different d_{MM}), which in practice can be done by appropriate instrumentation, the resulting transfer impedance variation can be directly attributed to the conductivity of the sample bands (Fig. 11b). It is seen in this figure that the transfer impedance magnitude decreases linearly with increasing sample conductivity, with the slope of the resulting traces representing perceptivity (i.e. the 'measurement sensitivity' - please see earlier footnote) [17]. The trace with the lowest d_{MM} value produces the line with

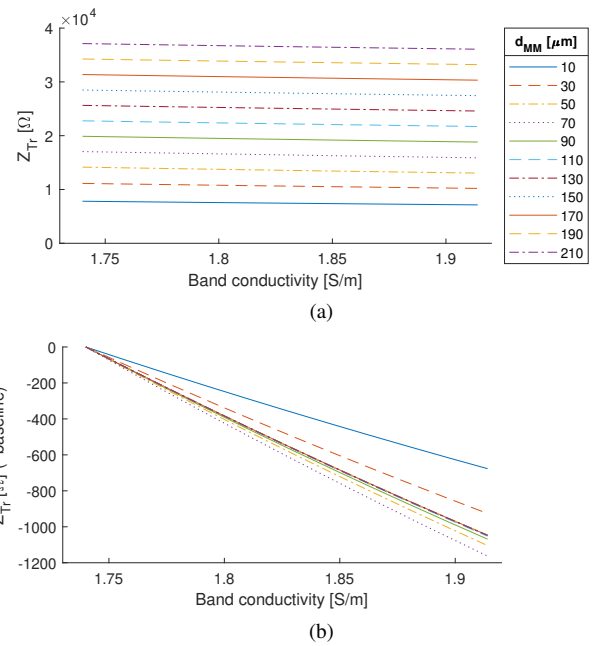


Fig. 11: Transfer impedance as a function of sample band conductivity for different values of the measurement electrode distance d_{MM} (a) raw data (b) with individual baseline subtraction

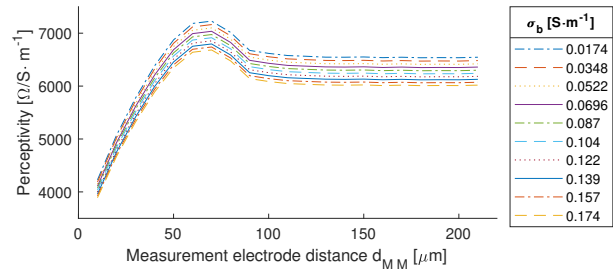


Fig. 12: Perceptivity calculated from transfer impedance as a function of measurement electrodes distance d_{MM} . Sample band length $l_b = 80 \mu\text{m}$, other dimensions as in Fig. 2

the smallest perceptivity (absolute slope). The relationship between perceptivity (slopes of the different traces in Fig. 11b) and d_{MM} is shown in Fig. 12 for each conductivity considered.

It is seen in this figure that the perceptivities for all conductivity variations considered increase with measurement electrodes' distance, peaking at $d_{MM} = 70 \mu\text{m}$, after which they recede to a plateau. That d_{MM} value is very close to the band length. This is a very significant result, as it indicates that the TEIM sensor should be designed with a particular d_{MM} in order to achieve maximum perceptivity. Therefore, while the previous results indicated that d_{MM} should be made as large as possible, this outcome indicates that an optimum value exists, possibly related to the band length. This is investigated in the following subsection.

E. Relationship between sample size and d_{MM}

As seen in Fig. 12 the perceptivity is largest for measurement electrode distances d_{MM} close to the length of the

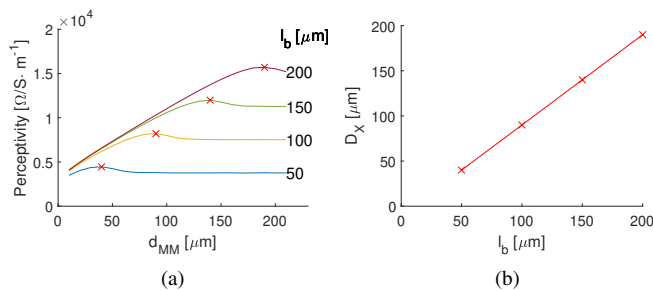


Fig. 13: (a) Perceptivity as function of measurement electrodes distance for sample bands ($\sigma_b = 0.174$ S/m) with different lengths at the tetrapole centre; red x indicates the maximum perceptivity at D_X (optimum d_{MM}); (b) D_X as a function of sample band length l_b

sample band length l_b , hence the sensor is acting as a spatial filter. In order to investigate the impact of d_{MM} on the sensor's perceptivity and spatial resolution, static sample bands ($\sigma_b = 0.174$ S/m) with four different sample lengths ($l_b = \{50, 100, 150, 200\}$ μm) positioned in the tetrapole centre were simulated.

Figure 13a shows that the d_{MM} value D_x at which perceptivity peaks (marked with a red marker) does depend on the sample band length. D_x may be called the optimum d_{MM} for a particular band length. Fig. 13b clearly demonstrates that the relationship between D_x and l_b is linear. D_x is smaller than l_b possibly due to the positive sensitivity region's borders extending slightly over each measuring electrode's edge (Fig.9). Therefore, in electrophoresis microfluidic chips employing TEIM sensors, d_{MM} should be designed to be slightly shorter (or even equal) to the projected sample length in order to achieve optimum performance, i.e. maximum perceptivity in band detection.

Based on the above, a design process can now - for the first time- be defined to optimise TEIM sensors for microfluidic channels. If the channel height, the channel width and the band length for a particular application width are known, an optimal sensor could be designed featuring the following: (a) L_X electrode length should be equal or longer than $2 \times h_{ch}$ with full width electrodes recommend for maximising the Z_{Tr} measurement; (b) D_X should be designed to be as close as possible to l_b of interest; (c) d_{II} is a parameter not affecting the result directly however placing the injection electrodes close to the measuring electrodes will reduce the overall sensor dimensions allowing it to be placed closer to the end of the separation channel, hence increasing the separation channel length.

V. CONCLUSION

A novel approach to methodically designing an optimised tetrapolar electrical impedance measurement (TEIM) sensor for microfluidic electrophoresis (ME) was presented here. The work was carried out through experimentally validated FEM simulations. The results show that a) highest perceptivity is obtained by an optimum choice of electrode length, while

keeping electrodes at a minimum size linearly related to the microfluidic channel height; b) the distance between the measuring electrodes should be proportional to the length of the analyte band to be detected and c) the distance between the current injection electrodes is indifferent. Another significant conclusion, interesting also beyond ME applications, is that - unlike what is observed in other TEIM applications - in microfluidic related measurements the negative sensitivity regions between the injecting and measuring electrodes are suppressed for small channel heights. Overall, by investigating the interrelation of channel, sensor electrodes and sample band dimensions a design process was developed leading to perceptivity improvements that indicate how bespoke impedimetric sensor design can optimise conductivity or impedance measurements in electrophoresis, without significant additional cost.

This study, as every modelling work that includes simplifications, exhibits some limitations and we wish to mention the main ones here to ensure that further research in this field takes these into consideration. The simulations carried out did not include five factors that are present in a practical ME setup: (a) the presence of the separation voltage - not really an issue if floating differential and ac coupled electronics are used; (b) electrode-related signal degradation due contact impedance - not an issue in TEIM - and thermal noise - similar across the designs examined; (c) interface electronics issues (e.g. current source output impedance, DC offsets etc) - all of which can be addressed through advanced circuit design; (d) fabrication tolerances - mostly eliminated through modern fabrication processes; and (e) absence of trains of moving bands - these were examined in our prior work which indicated the validity of the static band approach. Overall, the validity of the outcome of this work lies in the fact that all of these factors would be present - and thus would affect similarly - all of the TEIM sensor geometries examined. The outcomes of the work presented here indicate that using this methodology will pave the way for the widespread use of ME in POC diagnostic devices significantly increasing the options available for in-situ, rapid and portable diagnostics.

ACKNOWLEDGMENT

The authors would like to thank Genetic Microdevices Ltd. for financial and technical support.

REFERENCES

- [1] A. Wuethrich and J. P. Quirino, "A decade of microchip electrophoresis for clinical diagnostics: A review of 2008-2017," *Analytica Chimica Acta*, vol. 1045, pp. 42–66, 2019.
- [2] N. Nuchtavorn, W. Suntornasuk, S. M. Lunte, and L. Suntornasuk, "Recent applications of microchip electrophoresis to biomedical analysis," *Journal of Pharmaceutical and Biomedical Analysis*, vol. 113, pp. 72–96, 2015.
- [3] E. R. Castro and A. Manz, "Present state of microchip electrophoresis: State of the art and routine applications," *Journal of Chromatography A*, vol. 1382, pp. 66–85, 2015.
- [4] A. Wuethrich and J. P. Quirino, "Derivatization for separation and detection in capillary electrophoresis (2012-2015)," *Electrophoresis*, vol. 37, no. 1, pp. 45–55, 2016.
- [5] S. Grimnes, G. Martinsen, and G. K. Johnsen, "Mutual localization of electrode pairs in a 4-electrode measuring system," *Journal of Physics: Conference Series*, vol. 224, p. 12074, 2010.

- [6] K. Swinney and D. J. Bornhop, "Detection in capillary electrophoresis," *Electrophoresis*, vol. 21, no. 7, pp. 1239–1250, 2000.
- [7] S. Grimnes and G. Martinsen, *Bioimpedance and Bioelectricity Basics*, 2nd ed. New York: Academic Press, 2008.
- [8] F. Laugere, R. M. Guijt, J. Bastemeijer, G. V. D. Steen, A. Berthold, E. Baltussen, P. Sarro, G. W. K. V. Dedem, M. Vellekoop, and A. Bossche, "On-Chip Contactless Four-Electrode Conductivity Detection for Capillary Electrophoresis Devices," *Analytical Chemistry*, vol. 75, no. 2, pp. 306–312, 2003.
- [9] K. A. Mahabadi, I. Rodriguez, C. Y. Lim, D. K. Maurya, P. C. Hauser, and N. F. De Rooij, "Capacitively coupled contactless conductivity detection with dual top-bottom cell configuration for microchip electrophoresis," *Electrophoresis*, vol. 31, no. 6, pp. 1063–1070, 2010.
- [10] F. N. Moretti, J. L. Cabrera, and R. E. Madrid, "Zonal selectivity by sensitivity modulation in linear tetrapolar impedance sensors," *Sensors and Actuators, B: Chemical*, vol. 255, pp. 1268–1275, 2018.
- [11] T. Grysiński and Z. Morón, "Planar sensors for local conductivity measurements in biological objects Design, modelling, sensitivity maps," *Sensors and Actuators B: Chemical*, vol. 158, no. 1, pp. 190–198, 2011.
- [12] B. Graß, D. Siepe, A. Neyer, and R. Hergenröder, "Comparison of different conductivity detector geometries on an isotachopheresis PMMA-microchip," *Analytical and Bioanalytical Chemistry*, vol. 371, no. 2, pp. 228–233, 2001.
- [13] P. Kubá and P. C. Hauser, "Effects of the cell geometry and operating parameters on the performance of an external contactless conductivity detector for microchip electrophoresis," *Lab on a Chip*, vol. 5, no. 4, pp. 407–415, 2005.
- [14] K. Ansari, J. Y. S. Ying, P. C. Hauser, N. F. de Rooij, and I. Rodriguez, "A portable lab-on-a-chip instrument based on MCE with dual top-bottom capacitively coupled contactless conductivity detector in replaceable cell cartridge," *Electrophoresis*, vol. 34, no. 9–10, pp. 1390–1399, 2013.
- [15] M. Novotný, F. Opekar, and K. Štulík, "The effects of the electrode system geometry on the properties of contactless conductivity detectors for capillary electrophoresis," *Electroanalysis*, vol. 17, no. 13, pp. 1181–1186, 2005.
- [16] H. Zhang, X. Liu, H. Li, and X. Wang, "Effect of the detector parameters on the sensitivity of contactless conductivity detector for microchip electrophoresis," in *2008 Asia Simulation Conference - 7th International Conference on System Simulation and Scientific Computing*, 2008, pp. 355–358.
- [17] P. Tuma, F. Opekar, and K. Štulík, "A contactless conductivity detector for capillary electrophoresis: Effects of the detection cell geometry on the detector performance," *Electrophoresis*, vol. 23, no. 21, pp. 3718–3724, 2002.
- [18] P. Jacobs, A. Varlan, and W. Sansen, "Design optimisation of planar electrolytic conductivity sensors," *Medical & Biological Engineering & Computing*, vol. 33, no. 6, pp. 802–810, 1995.
- [19] D. B. Geselowitz, "An Application of Electrocardiographic Lead Theory to Impedance Plethysmography," *IEEE Trans. Biomed. Eng.*, vol. BME-18, no. 1, pp. 38–41, 1971.
- [20] B. H. Brown, A. J. Wilson, and P. Bertemes-Filho, "Bipolar and tetrapolar transfer impedance measurements from volume conductor," *Electronics Letters*, vol. 36, no. 25, pp. 2060–2062, 2000.
- [21] F. J. Pettersen, "On sensitivity in transfer impedance measurements," *Journal of Electrical Bioimpedance*, vol. 9, no. 1, pp. 159–162, 2018.
- [22] V. Silverio and S. de Freitas, "Microfabrication Techniques for Microfluidic Devices," in *Complex Fluid-Flows in Microfluidics*, F. J. Galindo-Rosales, Ed. Cham: Springer International Publishing, 2018, pp. 25–51.
- [23] S. D. Noblitt and C. S. Henry, "Improving the compatibility of contact conductivity detection with microchip electrophoresis using a bubble cell," *Analytical Chemistry*, vol. 80, no. 19, pp. 7624–7630, 2008.
- [24] E. X. Vrouwe, R. Lutgge, and A. van den Berg, "Direct measurement of lithium in whole blood using microchip capillary electrophoresis with integrated conductivity detection," *Electrophoresis*, vol. 25, no. 1011, pp. 1660–1667, 2004.
- [25] F.-J. Pettersen and J. O. Høgetveit, "From 3D tissue data to impedance using Simpleware ScanFE+IP and COMSOL Multiphysics a tutorial," *Journal of Electrical Bioimpedance*, vol. 2, no. 1, pp. 13–32, 2011.
- [26] M. Hantschke and I. F. Triantis, "Modeling the Impact of Sensitivity Distribution Variations of Tetrapolar Impedance Configurations in Microfluidic Analytical Devices," *IEEE Sensors Journal*, vol. 21, no. 2, pp. 1655–1664, 2021.
- [27] X. Liu, A. Demosthenous, and N. Donaldson, "Platinum electrode noise in the ENG spectrum," *Medical & Biological Engineering & Computing*, vol. 46, no. 10, pp. 997–1003, 2008. [Online]. Available: <https://doi.org/10.1007/s11517-008-0386-z>
- [28] M. Hantschke, D. Sideris, P. A. Kyriacou, and I. F. Triantis, "Optimization of Tetrapolar Impedance Electrodes in Microfluidic Devices for Point of Care Diagnostics using Finite Element Modeling," in *Proceedings of the Annual International Conference of the IEEE Engineering in Medicine and Biology Society, EMBS*, vol. 2018-July. IEEE, 2018, pp. 5321–5324.



Martin Hantschke received a Dipl. Ing. (BA) in Biomedical Engineering from Berufsakademie Bautzen in 2006. Between 2006 and 2016 he worked as an applied Biomedical Engineer in clinical settings. He received his MSc in Biomedical Engineering with Healthcare Technology Management from City, University of London in 2016. His MSc dissertation was on sensing methods in electrophoresis in collaboration with an industrial partner, Genetic Microdevices Ltd (GMD). Martin is currently carrying out research for his PhD at the Research Centre for Biomedical Engineering at City, University of London, focusing on spectrophotometric and conductive detection of electrophoretically separated carbohydrates. His PhD is part funded by GMD.



Iasonas F. Triantis is a Senior Lecturer at the Research Centre for Biomedical Engineering (RCBE), City, University of London. His main interests include multimodal neurostimulation methods; mental health diagnostic devices; impedimetric sensing in electrophoresis; reconfigurable electrodes for targeted diagnostics and impedance plethysmography. He has designed several analogue integrated circuits exploiting spatial properties of electrode topologies in electrical bio-interfaces. Previously (2010–12) he was a Senior Researcher at the Electronic and Electrical Engineering Department, UCL, focusing on front end ASICs for electrical impedance tomography (EIT). Between 2005–10 he was a Research Associate at Imperial College focusing on multi-modal neuroprostheses and vagus nerve interfaces. Between 2000–5 he was Research Assistant at UCL, where he received his PhD on implantable neural amplifiers. He received his MEng in Electronic Engineering from UMIST in 2000.